

Right hemisphere horizontal tuning during face processing

Justin Duncan^{1,2}, Guillaume Lalonde-Beaudoin¹, Caroline Blais¹ & Daniel Fiset¹

1. Département de Psychoéducation et Psychologie, Université du Québec en Outaouais
2. Département de Psychologie, Université du Québec à Montréal

Context

- Lesion¹ and neuroimaging² studies suggest that face processing is largely undertaken by right hemisphere cerebral regions.
- Behaviorally, superiority of the left visual field (LVF), i.e., the finding that faces are processed with greater speed and accuracy, vs. the right hemifield³, can be observed thanks to the separation of the visual fields along a vertical line that traverses the fovea⁴, and decussation of the visual pathways.
- Possible explanations include global/local⁵ and low/high spatial frequency⁶ processing specialization in the right (RH)/left (LH) hemispheres, respectively. Given the growing interest for spatial orientations in various aspects of face processing (detection⁷, identification⁸, emotion recognition⁹), we used orientation bubbles⁹ (**Figure 1**) to explore the processing of this facial information across the hemispheres.

Methods

- 37 participants, right-handedness verified with Edinburgh Inventory¹⁰, $\geq +60$ (7 excluded; final sample size $N = 30$),
- 18-33 years old ($M = 20.4$, $SD = 2.9$).

Learning phase

- Familiarization (max. 20 minutes);
- Blocks of 100 trials of a 10 AFC face identification task, whereby stimulus durations was reduced from 1,000ms to 500ms, to 250ms, to 120ms, and to 60ms, each time a block was completed with $\geq 90\%$ correct response.

Experiment 1 – Baseline orientation profiles

- 5 blocks X 100 trials of a 10 AFC face identification task;
- Stimulus duration was 60ms;
- Performance was maintained near 55% by adjusting the number of bubbles (i.e., quantity of signal) using QUEST¹¹.

Experiment 2 – Hemispheric orientation profiles

- 15 blocks X 40 trials (tot. 600, i.e., 300 trials/hemisphere) of a same/different task⁶ (see, for procedure, **Figure 2**);
- An orientation-filtered probe was presented unilaterally for 60ms (non-probe half was an average face distractor);
- Performance maintained near 75% across both hemispheres by adjusting the number of bubbles filtering the probe with QUEST;
- Eye-tracking was used to measure central fixation compliance ($M = 97.7\%$ of trials, $SD = 3.1\%$).

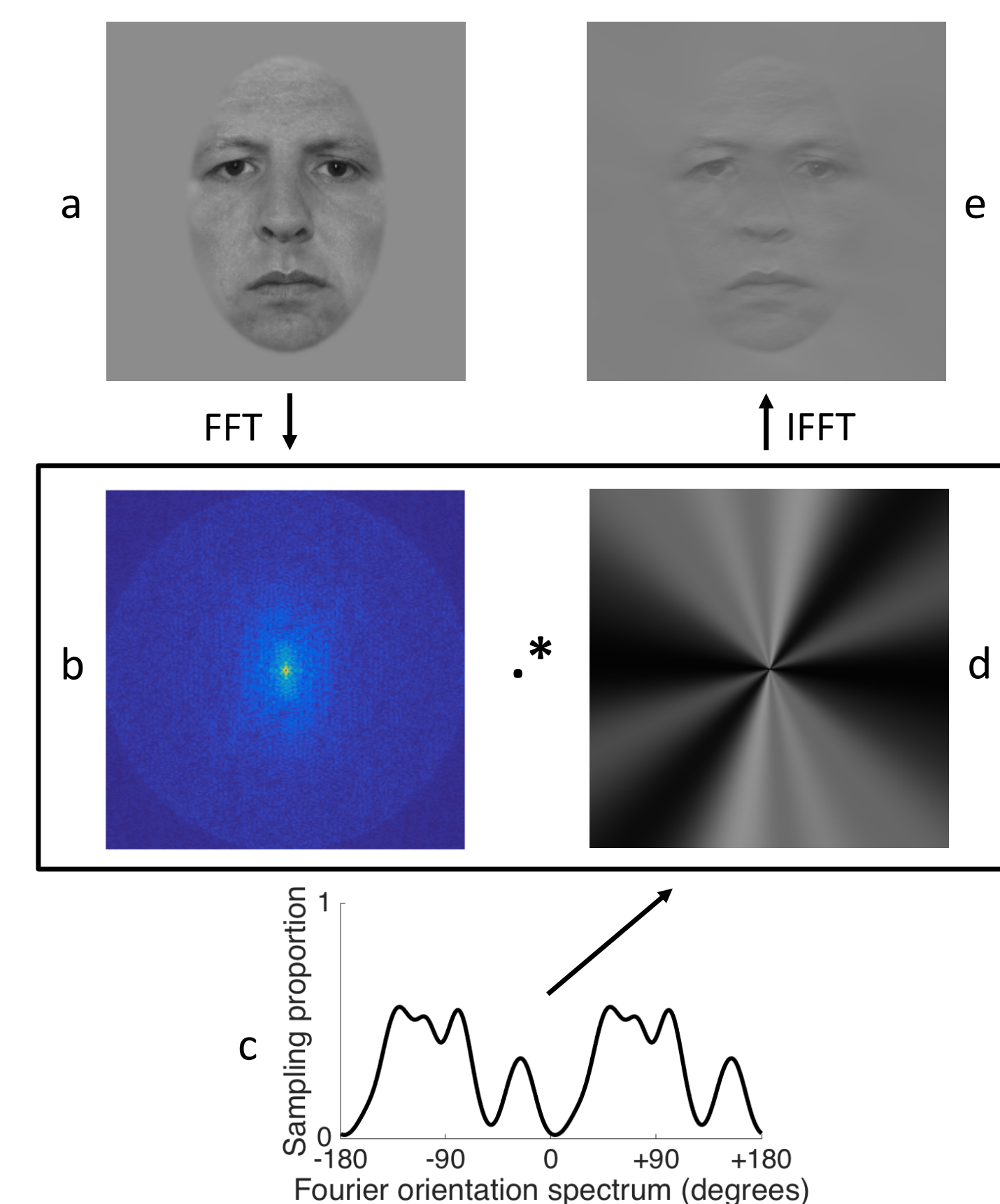


Figure 1. Orientation bubbles filtering procedure. The base image (a) orientation content is revealed by applying a Fast Fourier Transform (FFT) and shifting the resulting quadrants (b). An *orientation sampling vector* (c) comprising (here, 33) pairs of symmetrical Von Mises distributions is then converted to an *orientation sampling matrix* (d). The orientation matrix is applied to the image orientation content, and the filtered stimulus is reconstructed by inverse-FFT.

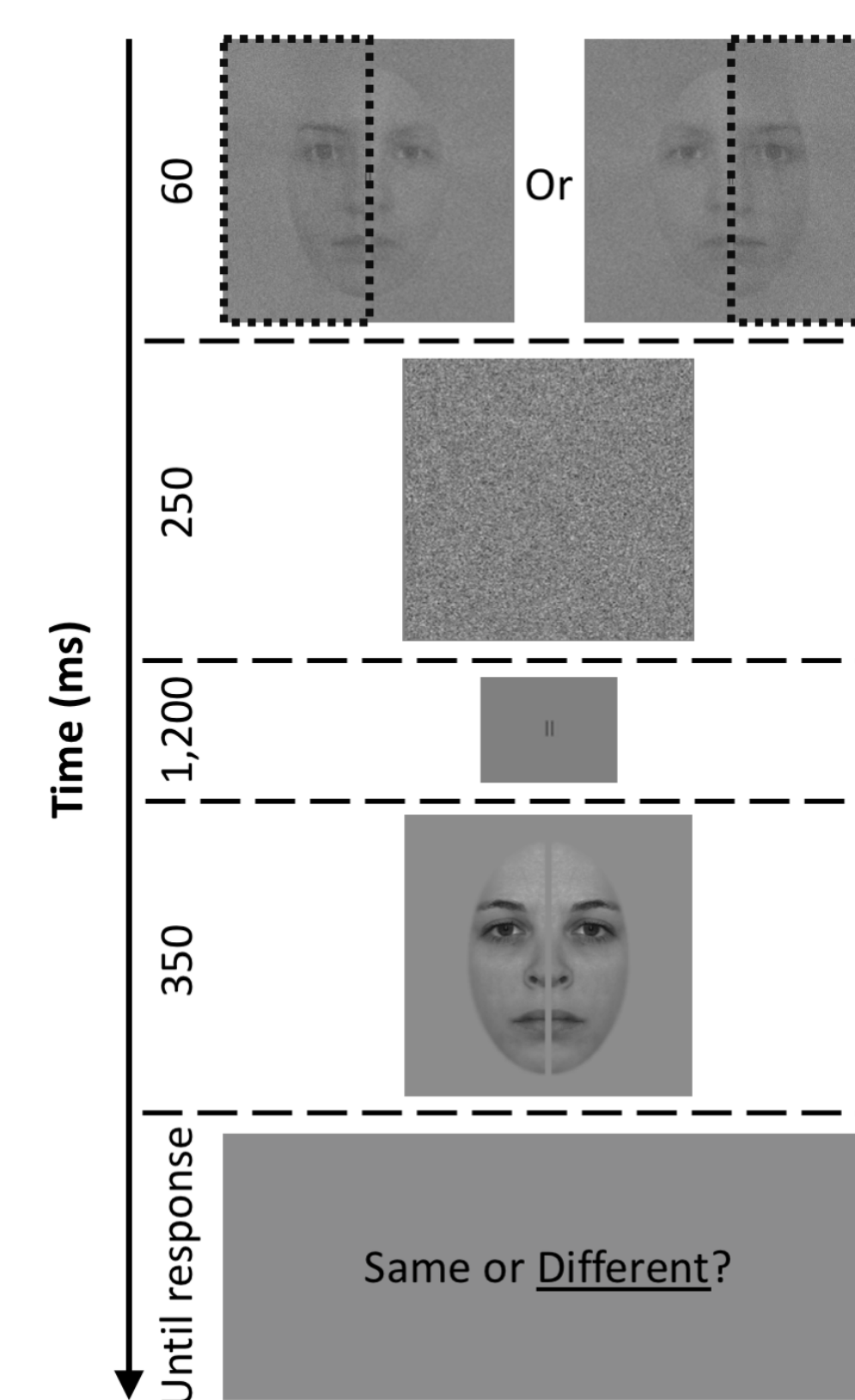


Figure 2. Experiment 2 trial. An orientation-filtered probe is presented (60ms) unilaterally (non-probe half is an average face distractor), followed by a noise mask (250ms), ISI (1,200ms), and broadband target (350ms). Subjects must tell if the probe and target are the same person or not.

Analyses and Results

- Orientation bubbles data were analyzed with a classification image analysis^{12, 13}: We calculated a weighted sum of orientation filters, allocating positive/negative weights (z-scored accuracies) to filters that led to correct/incorrect responses, respectively;
- Classification vectors were standardized using the mean and standard deviation of the null hypothesis⁹, summed to create a single group vector (divided by \sqrt{N}), and submitted to a pixel test¹⁴, $Z_{crit} = 2.1$, $p < .05$ (two-tailed), corrected for multiple observations.

Experiment 1

- 42.3 bubbles ($SD = 24.1$) were needed.
- Information around the horizontal axis [-92° to -56°] positively correlates with task accuracy (**Figure 3**), $Z_{max} = 3.38$, $p < 0.005$.

Experiment 2

- 44.4 bubbles ($SD = 15$) needed to maintain 81% ($SD = 5.6\%$) correct responses in the LVF/RH and 73.5% ($SD = 5.1\%$) in the RVF/LH, and the difference between hemifields was significant, $t(29) = 5.13$, $p < 0.001$, $d = 0.94$;
- Response times were also faster in the LVF ($M = 756\text{ms}$, $SD = 179$), vs. RVF ($M = 772\text{ms}$, $SD = 176$), $t(29) = 2.33$, $p < 0.05$, $d = 0.43$;
- For the LVF/RH, information around the horizontal axis [-93° to -54°] positively correlates with task accuracy (**Figure 4**, black), $Z_{max} = 3.45$, $p < 0.001$.
- For the RVF/LH however, horizontal information marginally negatively correlates with task accuracy (**Figure 4**, dark grey), $Z_{max} = -1.92$, $p < 0.1$.
- A direct comparison of the two profiles by subtraction (**Figure 4**, light grey) reveals significant differences around the horizontal ($[-97^\circ$ to $-64^\circ]$; $Z_{max} = 3.76$, $p < 0.001$) and vertical ($[-180^\circ$ to $-142^\circ]$; $Z_{min} = -2.85$, $p < 0.01$) axes.

Discussion

- The group orientation profile extracted from Experiment 1 confirms that horizontal information is diagnostic of face identification, and accuracy and speed data from Experiment 2 confirm that the LVF superiority in face processing was successfully replicated in this protocol;
- Orientation profiles extracted from Experiment 2 show that the LVF/RH, but not the RVF/LH, relies on diagnostic horizontal face structure—in fact, horizontal information marginally increased error rates in the RVF/LH;
- Thus, superiority of the LVF might emerge as a result of different orientation tuning across the hemispheres.

References

- (1) Mayer, E., & Rossion, B. (2007). In *The Behavioral and Cognitive Neurology of Stroke*, pp. 315-334; (2) Kanwisher, N., McDermott, J., & Chun, M.M. (1997). *The Journal of Neuroscience*, 17(11); (3) Sergent, J., & Bindra, D. (1981). *Psychological Bulletin*, 89(3); (4) Shilcock, R., Ellison, T.M., & Monaghan, P. (2000). *Psychological Review*, 107(4); (5) Rossion et al. (2000). *Journal of Cognitive Neuroscience*, 12(5); (6) Sergent, J. (1985). *Journal of Experimental Psychology: Human Perception and Performance*, 11(6); (7) Balas, B. J., Schmidt, J., & Saville, A. (2015). *Frontiers in Psychology*, 6; (8) Pachai, M.V., Sekuler, A.B., & Bennett, P.J. (2013). *Frontiers in Psychology*, 4; (9) Duncan, J., Gosselin, F., Cobarro, C., Dugas, G., Blais, C., & Fiset, D. (2017). *Journal of Vision*, 17(14); (10) Oldfield, R.C., (1971). *Neuropsychologia*, 9; (11) Watson, A.B., & Pelli, D.G. (1983). *Perception & Psychophysics*, 33(2); (12) Eckstein, M.P., & Ahumada Jr, A.J. (2002). *Journal of Vision*, 2(1); (13) Gosselin, F., & Schyns, P.G. (2004). *Cognitive Science*, 28(4); (14) Chauvin, A., Worsley, K.G., Schyns, P.G., & Gosselin, F. (2005). *Journal of Vision*, 5.

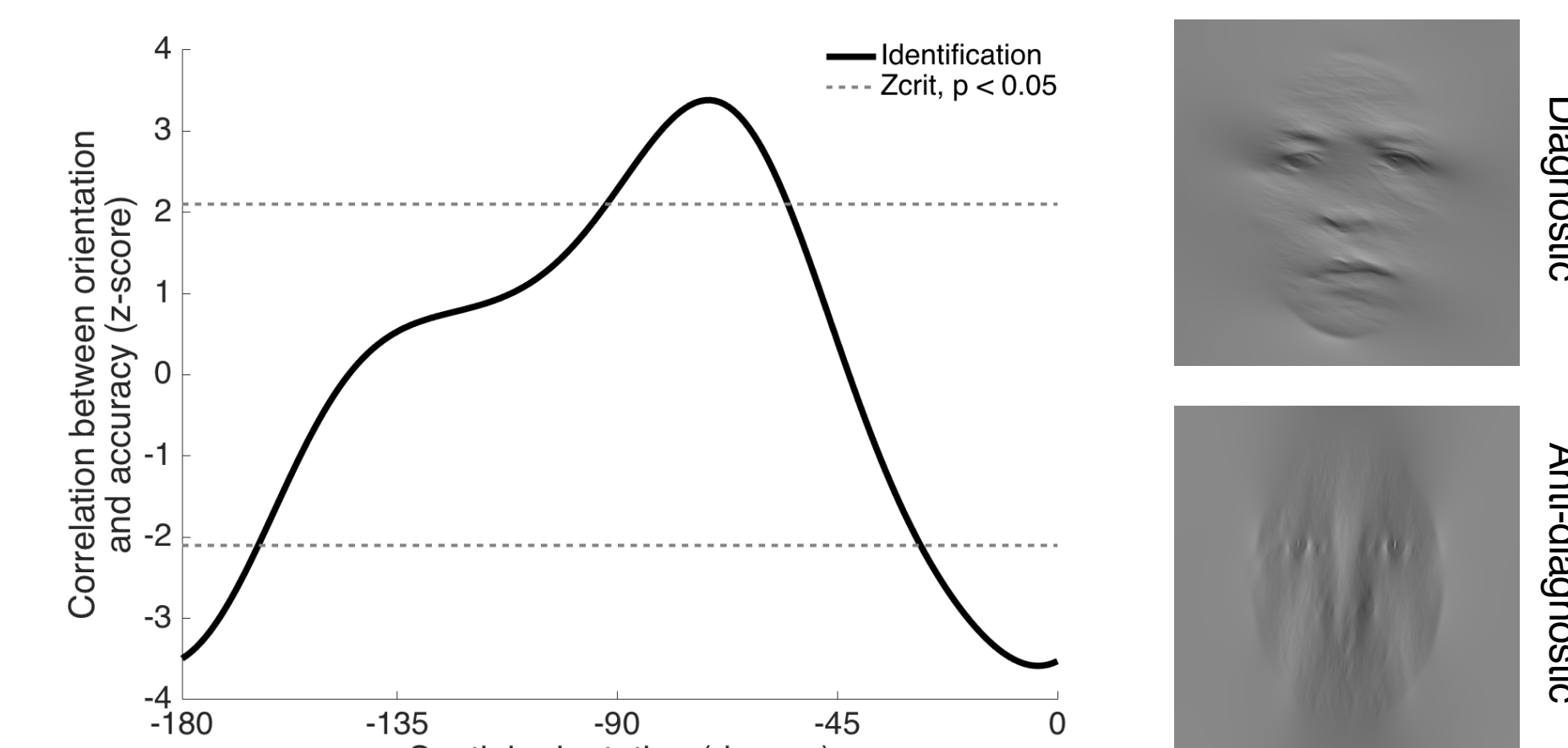


Figure 3. Experiment 1 results. (Left) Group classification vector illustrates the correlation (z-score) between orientation and task accuracy for face identification. Dotted lines plot the two-tailed significance threshold, $Z_{crit} = 2.1$, $p < 0.05$. (Right) Images filtered with diagnostic (top) and anti-diagnostic (bottom) orientations.

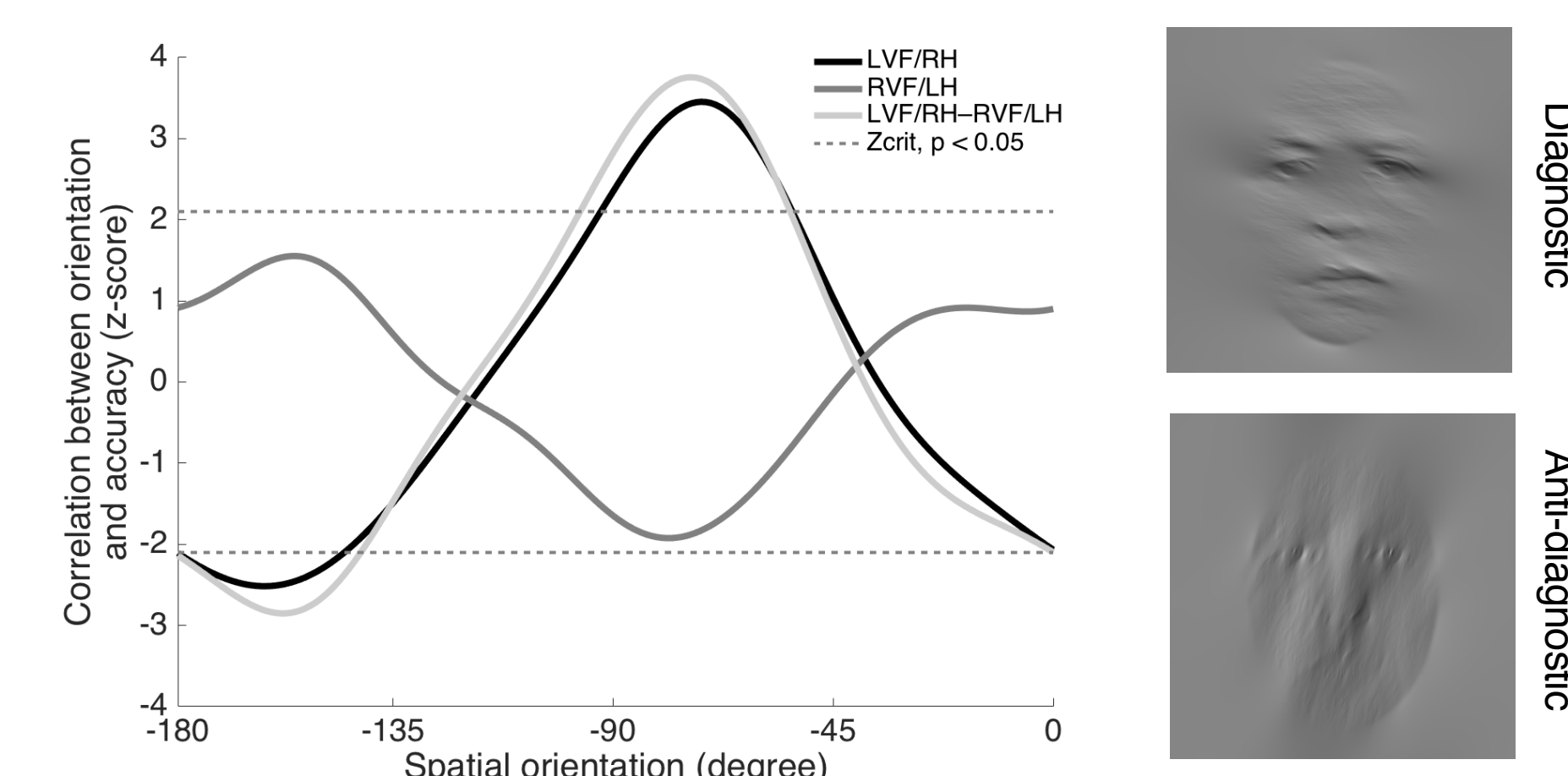


Figure 4. Experiment 2 results. (Left) Group classification vectors illustrating the correlation (z-score) between orientation and task accuracy in the left hemifield (black), and the right hemifield (dark grey); and the difference between both hemifields (light grey). Dotted lines plot the two-tailed significance threshold, $Z_{crit} = 2.1$, $p < 0.05$. (Right) Images filtered with diagnostic (top) and anti-diagnostic (bottom) orientations.